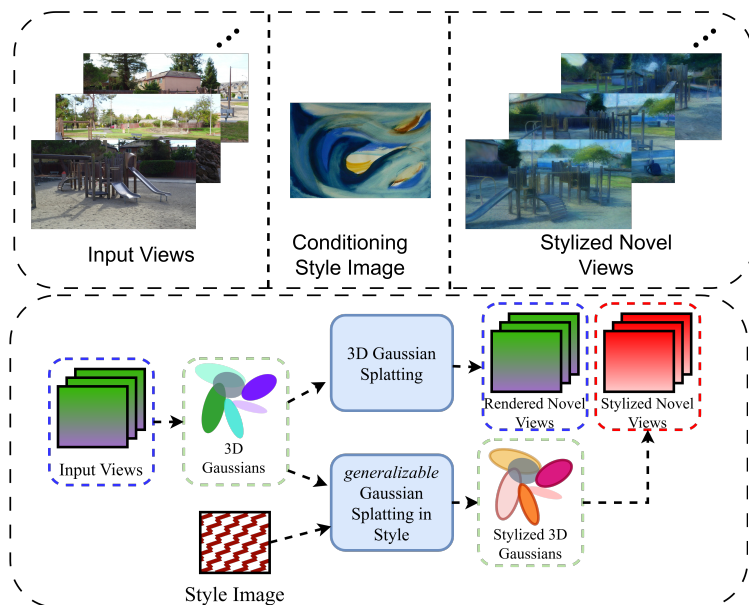


# Gaussian Splatting in Style

Abhishek Saroha<sup>1</sup>, Mariia Gladkova<sup>1</sup>, Cecilia Curreli<sup>1</sup>, Tarun Yenamandra<sup>1</sup>,  
and Daniel Cremers<sup>1</sup>

Technical University of Munich, Germany



**Fig. 1:** Given multi-view images of a real-world scene, we perform the task of scene stylization. We train a network that, provided with style image at test time, generates stylized novel views of the scene conditioned on the input style in real-time that are consistent in 3D space. In contrary to popular scene stylization approaches of fitting a scene with each new style, we learn this mapping via a neural network and therefore, can generate novel views of the scene even for unseen styles at a rate of roughly 150FPS.

**Abstract.** Scene stylization extends the work of neural style transfer to three spatial dimensions. A vital challenge in this problem is to maintain the uniformity of the stylized appearance across a multi-view setting. A vast majority of the previous works achieve this by optimizing the scene with a specific style image. In contrast, we propose a novel architecture trained on a collection of style images, that at test time produces high quality stylized novel views. Our work builds up on the framework of 3D Gaussian splatting. For a given scene, we take the pretrained Gaussians and process them using a multi resolution hash grid and a tiny MLP to obtain the conditional stylised views. The explicit nature of 3D Gaussians give us inherent advantages over NeRF-based methods including geometric consistency, along with having a fast training and rendering regime. This enables our method to be useful for vast practical use cases such as in augmented or virtual reality applications. Through our exper-

iments, we show our methods achieve state-of-the-art performance with superior visual quality on various indoor and outdoor real-world data.

**Keywords:** Scene Stylization · Gaussian Splatting

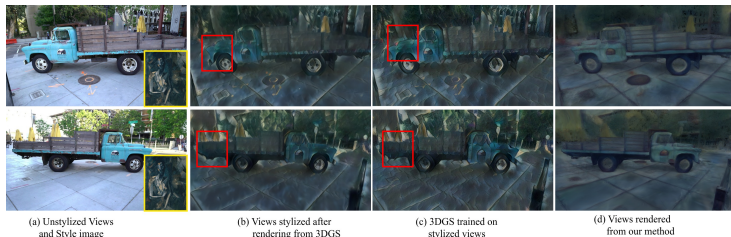


**Fig. 2:** The motivation from our work stems from the requirement of a specialized method that while stylizing a scene considers the spatial information into account. We show that to generate stylized novel views of a scene, it is not sufficient to stylize the rendered views or train a scene representation model on stylized 2D images. It leads to loss of information such as deformity in solid truck’s body shown above.

## 1 Introduction

Driven by the curiosity of how a particular image would appear if painted by Van Gogh, Picasso or any artist, style transfer has been at the heart of the image processing community for a long time. It can be seen as a challenge of texture transfer. Earlier works of [12, 13, 37, 81] devised powerful algorithms for texture synthesis. Further advancements in deep learning gave rise to works such as [16, 27, 31] that approach the problem by suitably trained neural networks. The core idea of neural style transfer is to apply the features of a style image such as colors, texture, and aesthetics to the content image while keeping information inside the content image intact. The ability of neural networks to grasp the features of an image at multiple hierarchical levels made them a preferred choice over non-learning based algorithms [16]. Fuelled by the availability of 3D data, this phenomenon of style transfer was extended to the stylization of scenes [26, 28, 43, 87], and is referred to as *scene stylization*.

In this work, we propose a solution for the task of scene stylization given a style image. The ability to control the visual properties of a scene is central to many practical applications such as avatar modeling or scene editing [51, 60, 64, 91] to name a few. With the wide adaptability of various augmented and virtual reality appliances gaining momentum, it is not only necessary that these techniques are correct, but also need to execute in real-time for maximum consumer satisfaction.

Over the past few years, various different methods have been proposed to efficiently represent a complex 3D scene. [59, 71, 77, 82] were some of the methods leveraging an explicit pointcloud representation. The domain witnessed an incredible pace of growth following the pioneering work of Neural Radiance Fields (NeRFs) [49, 50]. NeRFs gained large popularity, primarily due to its ability to store the information of a complex scene as the weights of a multi-layer perceptron (MLP), while maintaining great detailing in the resulting novel view synthesis. One drawback of radiance fields was the slow speed of training and at test

time. This was followed up by many variants of NeRFs such as [1, 3, 54, 57, 66, 86] that improved the seminal work significantly. Recently, the work of 3D Gaussian Splatting(3DGS) [33] further pushed the boundaries of novel view synthesis, especially in terms of consistency and speed. 3DGS is, by design, more explicit in terms of storing scene information in the form of 3D Gaussians, with each Gaussian having certain properties attached to it. Additionally, 3DGS renders views in real-time, thus making it highly suitable for practical applications.

In this paper, we tackle the problem of scene stylization as that of stylizing a set of pre-trained Gaussians given a set of style images. Therefore, we name our approach as Gaussian Splatting in Style(GSS). We then use these Gaussians conditioned on a style image to obtain stylized views of the complex 3D scene. Utilizing these Gaussians as the backbone of our approach ensures spatial consistency. Furthermore, our approach does not add any overhead to the existing real-time rendering speed of 3DGS, making it a preferred choice for applications in AR/VR ecosystems. We support our method by obtaining the most consistent short-term and long-term views as a quantitative metric. To further strengthen our approach, we also compare the superior quality of stylized novel views generated by our method in a qualitative fashion against other methods. To summarise, our contribution in this paper are as follows:

- We develop a novel state-of-the-art method, GSS, to perform neural scene stylization in real-time based on 3D Gaussian splatting. To the best of our knowledge, we are the first method to perform scene stylization using 3D Gaussians.
- We demonstrate the effectiveness of our method by comparing against various types of baselines both quantitatively and qualitatively across various real-world datasets across different settings.

## 2 Related Work

### 2.1 3D Scene representation

Complex 3D scenes can be represented in many ways. One of the most common and well known ways is that of using point clouds [2, 26]. Similar to point clouds, some works such as [69, 85] use a voxel grid for representing a 3D scene. Voxel grids are not the most ideal choice for scene representation due to their high memory footprint. Neural implicit scene based methods, led by the works of [46, 62, 63] making use of signed distance fields(SDFs) and occupancies respectively, helped solve this memory issue. In principle, implicit neural representations can generate meshes and surfaces upto an arbitrarily high resolution. Recently, work of NeuralAngelo [42] set a new benchmark as it could recover a highly detailed 3D surface of a large-scale scene from a set of input images. Following a similar direction neural radiance fields, also known as NeRFs [50] are also an implicit method that is described in further detail below.

## 2.2 Novel View Synthesis

The task of generating unseen views of an object/scene given a collection of input images is known as novel view synthesis. Classical works, such as [5, 10, 17, 22, 39, 70, 92] aimed at generating novel views directly from the given set of multi-view images. With the onset of deep learning, new approaches such as [21, 67, 73, 74] paved the way for neural network-based novel view synthesis(NVS). All these methods represented the scene in their own ways. A major milestone in the domain of NVS was with the advent of Neural Radiance Fields(NeRFs) [50]. NeRFs represent the scene as the weights of a multi-layer perceptron(MLP). The input to these MLPs are points in space and the viewing direction, which then gives out the density and color for each queried point. Despite its success, NeRF suffered from many drawbacks. A slow training regime, followed by the need to optimize it for each scene made it less viable for many use cases. It was also observed that NeRFs performed extremely well when the input views were dense and covered many angles of the scene. It often failed to get the finer details from views far-away from those used in training. Follow up works such as [9, 18, 57, 86] focused specifically on solving NVS for a sparse set of input views. Meanwhile, [55, 83, 86] focused on a more generalized framework to avoid fitting a MLP to each new scene, while [1, 54, 66, 85] improved on the original work in terms of training and inference speed. Recently, 3D Gaussian Splatting(3DGS) [33] also tackled the task of novel view synthesis in real-time. We explain the idea of 3DGS in Section 3 and can recommend the readers to visit [33] for more details.

## 2.3 Style Transfer

Neural style transfer is the task of transferring the style of a source image onto the target(or content) image [16]. It is a complex task as the transfer needs to preserve the information present in the target image. This problem can also be formulated as that of texture transfer, and was tackled in the works of [12, 13, 37, 81] before the widespread adoption of neural networks. Later, the pioneering work of [16] successfully applied the use of neural networks to the task of style transfer. The work made use of a pretrained VGG [72] to extract the semantic information from an image at different hierarchical levels. [16] optimized a loss function composed of two terms, content loss and style loss, which represented the similarity of the generated image with the content image and the style image respectively. The style loss was optimized by using the Gram matrix. The primary objective of Gram matrix was to encapsulate the correlations between the different features. Since [16] worked by running an optimization for each target and style image, it was not suitable for real-time applications. This was further improved by [27, 31, 40, 78] by being real-time and providing the flexibility of general style conditioning. Additionally, the works of [30, 44] added the sophistication of monocular depth estimation for preserving the depth information present in the source image. Furthermore, works of [4, 6, 15, 19, 25, 80] extended the work of 2D style transfer to a video sequence by making use of advancements

in methods like optical flow [11]. However, [26] and our experiments show that simply extending 2D style transfer to 3D scenes result in visual artifacts such as blurriness and inconsistency across different views, as also depicted in Chapter 1.

## 2.4 Scene Stylization

Stylizing scenes given a style image has gained prominence in recent years, especially with the arrival of AR/VR headsets in the mainstream. One way to distinguish between different methods is based on their way of scene representation. Works of [2, 26, 52] work with a point cloud based representation. [26] for instance, project the style features from 2D into 3D and transform them into that of the style image before re-projecting them back into 2D for getting stylized views. Similarly, [23] performs scene stylization of indoor scenes in the form of a mesh. Recently, radiance fields [50] gained huge popularity due to their ability to generate novel views with a very high quality. Due to this, a lot of works made use of a NeRF backbone to perform scene stylization. One direction of approaching the problem is by focusing to optimize a radiance for each given style image. Methods such as [8, 32, 41, 56, 61, 84, 87, 89, 90] follow this outline. Methods such as [7, 8] make use of a hypernetwork to impart the style image features onto the rendered views of a complex 3D scene. On the other hand, works such as [28, 43] provide a generalizable scene stylization framework, i.e a stylized scene can be generated at inference time given a conditioned style image input. Our work also follows in this category. Another direction in this domain lies making use of additional information such as depth maps [32] since their primary focus lies in geometry preservation. In this work, instead of a radiance field, we make use of a Gaussian splatting [33] framework. To the best of our knowledge, we are the first method that builds up on a 3DGS backbone for image-based scene stylization.

Apart from image based conditioning for stylization, one direction is to input the conditioning in the form of text. Leveraging the use of large language models (LLMs), [14, 20, 29, 47, 48, 75, 79] perform scene editing, and stylization in some cases, via text-based inputs. In our work, we do not compare with any text-based input methods and focus entirely on methods that condition the scene via style images only. While textual information can be informative and descriptive, the challenges of image-based conditioning can be far more demanding as it provides information in terms of abstraction, strokes, and so on.

## 3 Preliminaries

### 3.1 3D Gaussian Splatting

3D Gaussian Splatting (3DGS) [33] is an explicit method for scene representation, that is especially useful for high quality real-time rendering. It can be considered as a form based on point cloud representation. Each scene in 3DGS is represented as a bunch of 3D Gaussians, each of which has certain properties. Each 3D Gaussian is defined by its mean position  $\mu \in \mathbb{R}^3$ , covariance matrix  $\Sigma$  as the following:

$$G(X) = e^{-\frac{1}{2}\mu^T \Sigma^{-1} \mu}. \quad (1)$$

Since the covariance matrix has to be positive semi-definite for differentiable optimization, it is decomposed into a rotation matrix  $\mathbf{R}$ , expressed in quaternions and a scaling matrix  $\mathbf{S} \in \mathbb{R}^3$  as:

$$\Sigma = \mathbf{R} \mathbf{S} \mathbf{S}^T \mathbf{R}^T. \quad (2)$$

Additionally, each Gaussian also contains the opacity  $\alpha$  and view-dependent color values, represented by spherical harmonics coefficients. Once initialised, these Gaussians are projected onto 2D for rendering. This rendering process is done by a differentiable tile rasterizer. During the process of optimization, these Gaussians undergo density control, i.e they are constantly removed and new ones are added to the scene in order to maintain high image quality. This is done in order to ensure that the density of Gaussians is more or less consistent in all areas of the scene, especially ones which were empty during the SfM initialization. The 3D scene is optimized for the following loss function:

$$\mathcal{L} = (1 - \lambda)\mathcal{L}_1 + \lambda\mathcal{L}_{D-SSIM} \quad (3)$$

where  $\mathcal{L}_1$  and  $\mathcal{L}_{D-SSIM}$  are computed between the generated image and the ground truth view. For thorough explanation, we refer the reader to [33].

### 3.2 Multi-resolution Hash Grid

Encoding neural network inputs into higher dimensional space has been crucial in achieving scene representations of high quality with compact models [50]. [54] furthers fidelity and efficiency by outsourcing the representation power to an auxiliary data structure, namely a multi-resolution hash grid, which allows fast access to learned features at each grid cell on multiple spatial resolutions. Specifically, an input 3D point is first parameterized by a hash code  $(\mathbf{x}_1, \dots, \mathbf{x}_l)$ , which corresponds to the corner indices of a set of grids with different spatial resolution  $\{V_1, \dots, V_L\}$ . Given those indices, feature vectors are obtained and linearly interpolated according to the relative position of  $\mathbf{x}$  across all  $L$  spatial resolutions. Formally, the final multi-resolution hash encoding of a 3D point  $\mathbf{x}$  becomes  $\gamma(\mathbf{x}) = (\gamma_1(\mathbf{x}_1), \dots, \gamma_l(\mathbf{x}_l))$ , where  $\gamma_l(\mathbf{x}_l)$  is a feature vector obtained by means of interpolation of hash entries at the grid corners of the  $l$ th resolution level.

Multi-resolution hash encoding is independent at each level and highly adaptive to the desired finest resolution. Thus, it enables faster convergence during training, does not impede inference speed, and promotes a higher level of detail, which is beneficial for the stylization task using 3DGS representation.

### 3.3 Stylized NeRF

StylizedNeRF [28] set up a new benchmark in the field of neural scene stylization. Built upon the framework of NeRF and Nerf-W [45, 50], this work makes use of a

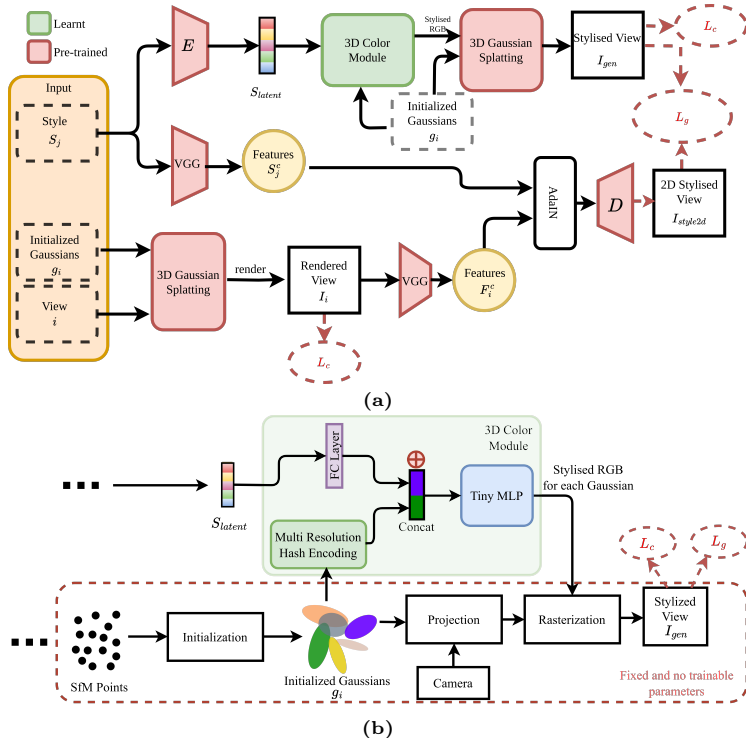


**Fig. 3:** Here we diagrammatically show the overall architecture of our pipeline. (a) contains the overview of our method. (b) shows in detail the top-right part of (a) where we have a deeper look into how the 3D color module combines with 3DGS to produce stylized novel views.

mutual learning strategy to combine 2D stylization method AdaIN [27] and a pre-trained NeRF architecture. The high-level idea is to predict a new stylized color conditioned on the style image. This is achieved by replacing the color component with a new style module while keeping the density prediction from the pre-trained NeRF constant to maintain geometric consistency. To facilitate mutual learning between 2D-3D stylization, StylizedNeRF makes the decoder of AdaIN trainable for fine-tuning the final results. Inspired by Nerf-W, they also employ a pre-trained VAE that provides learnable latent codes for the conditioned style inputs. Motivated by the positive results of StylizedNeRF, GSS also makes use of pre-trained Gaussians to better represent the geometric details of the complex scenes.

## 4 Gaussian Splatting in Style

Our goal is to stylize a complex 3D scene. The first step is to learn the scene information from a given collection of images in a multi-view setting. We achieve

this by using a 3DGS backbone. For this objective, we take pretrained models of learnt scenes for the next step. The second stage includes learning the scene information conditioned on various style images. During inference time, we generate novel views conditioned on an input style image. In the following section, we elaborate on the various constituents of our pipeline.

**2D Stylization Module** The first component of our pipeline is a 2D stylization module. It is based on AdaIN [27]. It consists of three components, a pretrained VGG [72] as the encoder, a convolutional decoder, and adaptive instance normalisation layer. For details, please refer to [28]. As shown in Figure 3, we pass the style image and the rendered view from 3DGS through a pretrained VGG to obtain their features. These features are then passed through the adaptive instance normalization layer and the decoder to obtain the 2D styled image of that particular view. This 2D stylized image acts as a guide for our 3D color module, and gives a rough indication as to how the scene should appear from that specific viewpoint. Therefore, this image, represented by  $\mathcal{I}_{style2d}$  forms on what we call it as a Guide Loss  $\mathcal{L}_g$ , which is detailed in Section 4.

**3D Color Module** This module is the second component in our overall architecture. The input to this module are the mean positions  $\mu$  of the 3D Gaussians and a latent code representing the style image obtained through the use of a pretrained encoder [28, 65]. The input positions are fed into a multi-resolution hash grid(MHG) [54] while the latent codes are fed into an FC layer before concatenating them together. This resulting tensor is then passed through a tiny MLP [38, 53] to obtain the new RGB color for each input Gaussian. The use of MHG and tiny MLP was motivated by the fact that each scene has a large number of Gaussians, and could also be in the order of millions for large scenes such as those in the TnT [35] dataset. The predicted RGB from the 3D color module is fed into the 3DGS pipeline, and the Gaussians, with their new colors are rendered to generate a 3D consistent stylised view  $\mathcal{I}_{gen}$ . To preserve important details in the scene, we compare  $\mathcal{I}_{gen}$  with the unstyled view  $\mathcal{I}_i$  as shown in Equation (5). Since our color module is view dependent, it does not affect the runtime during inference time. Since the geometry is conserved, one forward pass through GSS with the conditioned style input allows us to obtain the stylized RGB for any arbitrary viewpoint.

**Loss function** As shown in Figure 3, we apply the loss functions on the views generated by the 3D color module. Our loss term is composed as a weighted sum of two terms, the **guide loss**  $\mathcal{L}_g$  and the **content loss**  $\mathcal{L}_c$ , elaborated as follows:

$$\mathcal{L}_g = ||\mathcal{I}_{style2d} - \mathcal{I}_{gen}|| \quad (4)$$

$$\mathcal{L}_c = ||\mathcal{I}_{gen} - \mathcal{I}_i|| \quad (5)$$



where  $\mathcal{I}_{style2d}$ ,  $\mathcal{I}_i$ ,  $\mathcal{I}_{gen}$  are the 2D stylized image from the 2D stylization module, the unstyled view generated from 3D Gaussian splatting, and the stylized view from our pipeline respectively.

Finally, our total loss  $\mathcal{L}_{total}$  can be written as:

$$\mathcal{L}_c = \lambda_g \mathcal{L}_g + \lambda_c \mathcal{L}_c \quad (6)$$

where  $\lambda_g$  and  $\lambda_c$  are the weights of the guide loss and content loss respectively.

## 5 Experiments

Dataset ↓	Method →	GS → AdaIN	AdaIN → GS	LSNV	ARF	Stylised- NeRF	StyleRF	GSS(Ours)
Flower	RMSE ↓	0.098	0.083	0.030	0.036	0.002	0.038	0.034
	LPIPS ↓	0.106	0.080	0.011	0.015	0.001	0.013	0.009
Fern	RMSE ↓	0.127	0.116	0.075	0.038	0.041	0.037	0.026
	LPIPS ↓	0.151	0.134	0.049	0.020	0.012	0.019	0.008
Room	RMSE ↓	0.104	0.103	0.044	0.037	0.029	0.035	0.021
	LPIPS ↓	0.109	0.105	0.014	0.014	0.011	0.014	0.006
Trex	RMSE ↓	0.136	0.099	0.089	0.043	0.015	0.045	0.010
	LPIPS ↓	0.136	0.087	0.033	0.022	0.004	0.017	0.003

**Table 1: Short Term Consistency** Here, we demonstrate the superior performance of our method using the short-term consistency metric. We compute the metric using both, RMSE and LPIPS [88] using a VGG backbone. As shown in Figure 4, the novel views rendered by StylizedNerf are highly blurry and misses crucial details. Therefore, due to the over-smooth and blurry output, the metric obtained for them is really low and does not correctly reflect the adequate stylization qualities.

**Implementation Details** We build our work on top of the 3DGS [33] framework and use it to pretrain the Gaussians for each scene. For this, we followed the original training regime as suggested by the authors. For the 2D stylization module, we use a pretrained VGG [16, 72] and AdaIN [27] decoder. For obtaining the latent code of input style images, we use a pretrained image encoder used in [65]. As for the hyperparameters, we set  $\lambda_g$  and  $\lambda_c$  as 1 and 0.1 respectively. We train the tiny MLP for the second stage as per the training regime described in Figure 3 for 50k iterations. For optimization, we use the Adam [34] optimizer with a learning rate of  $1e^{-4}$ . We run all our experiments on a Nvidia A4500 GPU.

**Baselines** Since no previous approach performs scene stylization based on Gaussian splatting, we compare our method with NeRF-based approaches. We primarily compare against StylizedNerf [24, 28], and LSNV [26] as their problem statement resembles most closely to that of ours. We also compare against a newer method StyleRF [43], along with artistic radiance fields (ARF) [87], although ARF optimizes every scene for each given style image. For completeness, we also create two other baselines, ADA-GS and GS-ADA. In ADA-GS, we train 3DGS on 2D stylized images for each style. This setting resembles that of ARF.

In GS-ADA, we apply AdaIN [27] on the novel view renders obtained from pre-trained 3DGS.

**Datasets** Similar to the baselines [26, 28, 43] we perform stylization on various real-world datasets. For real-world, we use the LLFF dataset [49]. It contains high-resolution front-facing scenes, out of which we select the most common ones used in the baselines, namely *trex*, *fern*, *flowers*, *room*. We also demonstrate the effectiveness of our method on more challenging Tanks and Temples(TnT) [36] dataset. For training, we use a dataset of 120 diverse style images sampled from WikiArt dataset [68], which include the paintings and popular artworks of various artists.

Dataset ↓	Method →	GS → AdaIN	AdaIN → GS	LSNV	ARF	Stylised- NeRF	StyleRF	GSS(Ours)
Flower	RMSE ↓	0.147	0.141	0.040	0.123	0.002	0.123	0.090
	LPIPS ↓	0.151	0.135	0.018	0.112	0.001	0.081	0.057
Fern	RMSE ↓	0.151	0.132	0.076	0.109	0.044	0.115	0.042
	LPIPS ↓	0.193	0.162	0.051	0.107	0.019	0.099	0.021
Room	RMSE ↓	0.143	0.150	0.045	0.084	0.045	0.078	0.033
	LPIPS ↓	0.182	0.184	0.019	0.061	0.028	0.046	0.015
Trex	RMSE ↓	0.164	0.131	0.091	0.092	0.030	0.091	0.020
	LPIPS ↓	0.194	0.137	0.050	0.081	0.016	0.057	0.007

**Table 2: Long Term Consistency** In this table, we measure the performance of GSS against the said baselines via long-term consistency. Similar to [43], for long-term consistency, the two frames should be far away from each other. Having a long-term consistent method ensures that the produced novel views of the scene are consistent in the stylized color space. Similar to short-term consistency in Table 1, StylizedNerf numbers does not accurately depict the stylization quality as compared to other methods.

## 5.1 Quantitative Results

Since the task of scene stylization is relatively new, there are not many ways to quantitatively compare methods. However, following [26, 28, 43], we measure the quantitative result by measure short-term and long-term consistency. Similar to the evaluation in [43], we first take two stylized views. By using [76] and [58], we then warp one view into another before computing the masked LPIPS [88] and RMSE score. We use adjacent views for short-term and far-away views for long-term consistency. Many works such as [26] also refer to it as warped LPIPS and warped RMSE. Mathematically, they can be summarised as follows:

$$\mathbb{E}_{wlpips}(\mathcal{O}_v, \mathcal{O}_{v'}) = LPIPS(\mathcal{O}_v, \mathcal{M}_v(\mathcal{W}(\mathcal{O}_{v'}))) \quad (7)$$

$$\mathbb{E}_{wrmse}(\mathcal{O}_v, \mathcal{O}_{v'}) = RMSE(\mathcal{O}_v, \mathcal{M}_v(\mathcal{W}(\mathcal{O}_{v'}))) \quad (8)$$

where  $\mathcal{M}_v$ ,  $\mathcal{O}_v$ , and  $\mathcal{W}$  are the masking, view  $v$ , and the warping function respectively.

We quantitatively compare our method with the baselines as shown in Tables 1 and 2. It can be clearly seen that our method outperforms all other baselines in both short-term and long-term consistency. We can see that simply applying 2D stylization to rendered novel views is not enough to ensure consistency, in accordance with [26], and hence Ada-GS is almost always more consistent than GS-ADA for both short-term and long-term views. Furthermore, simply adding 2D stylization to the input or outputs of existing scene representation approaches is not sufficient, as all other dedicated baselines perform better on average than GS-ADA and ADA-GS. We also find that methods utilising explicit scene representations, such as GSS and LSNV [26] perform better than radiance field based baselines. It is also important to observe that for Stylized-Nerf, the generated novel views suffer from high blur, over-smoothing and loss of details. Due to this, they obtain a very high consistency despite not being of reasonable quality as compared to all other methods.

	LSNV	ARF	StylizedNerf	StyleRF	GSS
Rendered FPS	40	1	0.004	0.04	<b>157</b>

**Table 3:** We perform a runtime analysis of our method vs other baselines. Due to our 3DGS backbone, we are able to generate stylized novel views approximately 4x faster than the second method, achieving an average of 157 FPS(Frames per second). Radiance fields in general have a high rendering time and suffer from slow training and testing time.

On running on the same hardware, GSS is also the fastest. Whereas all other methods take in the order of a few seconds to minutes to generate a single view, we obtain a rendering speed of roughly averaging **157 FPS**. Our method is also very efficient in training and it requires roughly 2 hours to train for each scene on a standard Nvidia A4500 GPU.

## 5.2 Qualitative Results

Along with the quantitative results, we demonstrate the performance of our method with the baselines with a qualitative evaluation as shown in Figure 4. It can be seen that not only our method preserves content details better, it also is more faithful to the style images. For instance, while StyleRF [43] is great at preserving geometric details, it does not adequately transfer the style image features onto the novel views. On the other hand, ARF [87] is aggressive at transferring the style image features onto the scene, and hence often leads to a loss in the information. It also has an affinity to focus more on the central object and does not transfer the style to far-away objects in the scene. It is worth noting that ARF optimizes each scene for every style image. We also observe that StylisedNerf [28] produces blurry views while LSNV also struggles to retain fine details in the stylized views.

## 6 Ablation Studies

To study the effects of various components of our method, we perform several experiments and report their findings below.

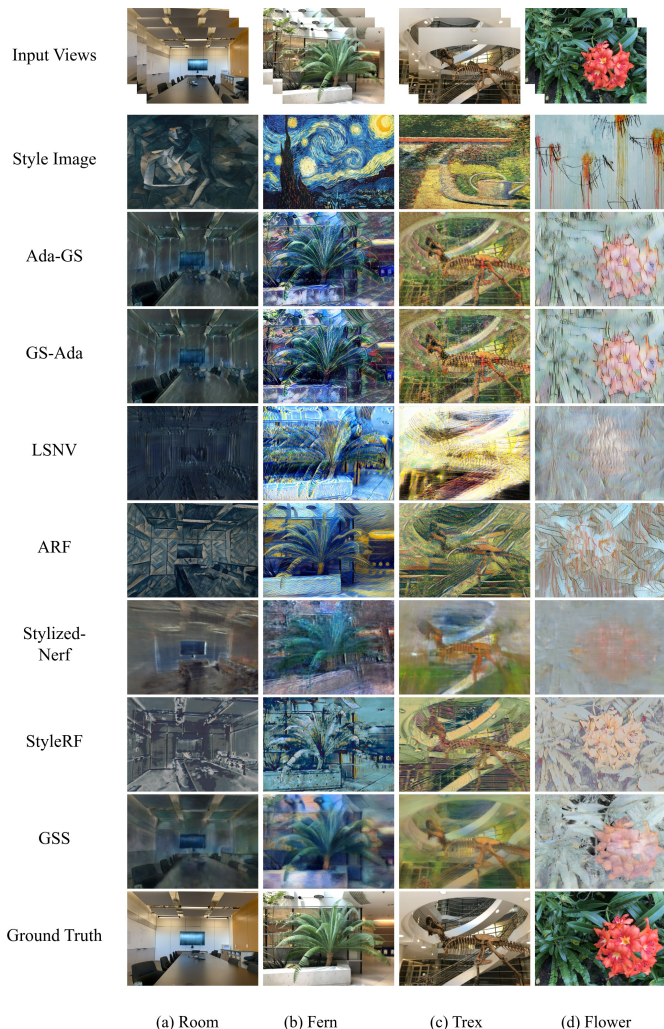


**Fig. 4:** We provide a detailed qualitative comparison of our method against the baselines detailed in Section 5. It can be seen that GSS achieves a highly accurate stylization based on the input style. While methods such as ARF obtain a better texture, it is attributed to the fact that it is optimized separately for each style. GS-Ada and Ada-GS are also able to get high quality texture, however, it is not accurate at geometry conservation since these methods are based on pure 2D stylization. Also, methods such as StyleRF fail to grasp the accurate style color such as that in room, fern or flower scene.

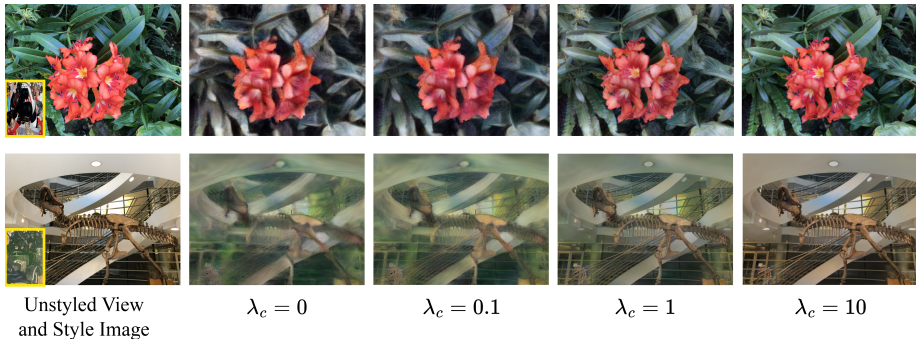


**Fig. 5:** Here we show the effect of varying  $\lambda_c$  in our loss function as described in Equation (5). We observe that setting  $\lambda_c = 0$  results in loss of details such as the anthers and filaments of the flower as shown above. However, further increasing  $\lambda_c$  results in loss of style, and the generated view looks similar to that of the unstyled view.

## 6.1 Content Loss

We first ablate the content loss  $\mathcal{L}_c$ , described in Equation (5), by varying the value of  $\lambda_c$ . We vary the value in the discrete set of  $\{0, 0.1, 1, 10, 100\}$  to cover a wide range of possible values.

Setting the value of  $\lambda_c = 0$  leads to over-smoothing of the generated view. While the generated view is still consistent and stylized, it loses some of the finer details. On increasing the value beyond 1, the rendered view resembles that of being unstyled.

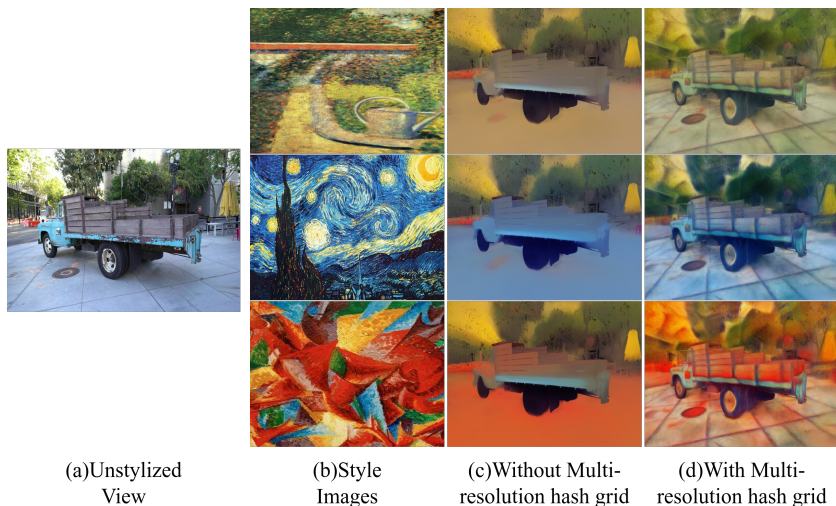


**Fig. 6:** We ablate the effect of multi-resolution hash grid(MHG) in our setup. We find that having MHG in our model enforces a much better texture and color transfer from the style image onto the scene. It can be attributed to its high capability of learning features, while keeping the model fast and small.

## 6.2 Multi-resolution Hash Grid

We also study the effect of having a multi-resolution hash grid(MHG). On removing the MHG from our 3D color module, we find that the resulting stylized scene is not adequately transferred onto the scene as shown in Section 6.1. Instead, the scene loosely adopts the color-palette from the style image without grasping any textual information, thus verifying our decision to use MHG.



**Fig. 7:** We interpolate between the latent vectors of the style images. The four style images are shown at the four corners of the image above and were chosen so they’re highly diverse and accurately depict the differences in the predicted RGBs for each Gaussian from our model.

## 6.3 Style Interpolation

We perform style interpolation by taking four different style images at test time, and obtaining the resulting style latent by linearly interpolating between the different styles. We show the results in Section 6.2. The ablation shows the capability of our model to generate results for not only the given style images, but also a mixture of such styles. It demonstrates that our model learns the mapping from style inputs to predicted RGB values for each 3D Gaussian in a meaningful way, and thus provides increased generalisability.

## 7 Conclusion

In this paper, we presented a novel method to stylize complex 3D scenes that are spatially consistent. Contrary to a majority of existing works, once trained, our method is capable to take unseen input scenes at inference time and produce novel views in real-time. By leveraging a multi-resolution hash grid and a tiny MLP, we are able to accurately generate the stylized colors of each 3D Gaussian present in a scene. Since we only do one forward pass through the 3D color module, we are able to generate novel views at around **150FPS**. We exhibit that GSS produces superior results by the use of quantitative and qualitative results, thus making GSS suitable for many practical applications.

## References

1. Barron, J.T., Mildenhall, B., Tancik, M., Hedman, P., Martin-Brualla, R., Srinivasan, P.P.: Mip-nerf: A multiscale representation for anti-aliasing neural radiance fields (2021) [3](#), [4](#)
2. Cao, X., Wang, W., Nagao, K., Nakamura, R.: Psnnet: A style transfer network for point cloud stylization on geometry and color. In: Proceedings of the IEEE/CVF Winter Conference on Applications of Computer vision. pp. 3337–3345 (2020) [3](#), [5](#)
3. Chen, A., Xu, Z., Geiger, A., Yu, J., Su, H.: Tensorf: Tensorial radiance fields. In: European Conference on Computer Vision (ECCV) (2022) [3](#)
4. Chen, D., Liao, J., Yuan, L., Yu, N., Hua, G.: Coherent online video style transfer. In: Proceedings of the IEEE International Conference on Computer Vision. pp. 1105–1114 (2017) [4](#)
5. Chen, S.E., Williams, L.: View Interpolation for Image Synthesis. In: SIGGRAPH (1993) [4](#)
6. Chen, X., Zhang, Y., Wang, Y., Shu, H., Xu, C., Xu, C.: Optical flow distillation: Towards efficient and stable video style transfer. In: Computer Vision–ECCV 2020: 16th European Conference, Glasgow, UK, August 23–28, 2020, Proceedings, Part VI 16. pp. 614–630. Springer (2020) [4](#)
7. Chen, Y., Yuan, Q., Li, Z., Liu, Y., Wang, W., Xie, C., Wen, X., Yu, Q.: Upst-nerf: Universal photorealistic style transfer of neural radiance fields for 3d scene (2022) [5](#)
8. Chiang, P.Z., Tsai, M.S., Tseng, H.Y., sheng Lai, W., Chiu, W.C.: Stylizing 3d scene via implicit representation and hypernetwork (2022) [5](#)
9. Chibane, J., Bansal, A., Lazova, V., Pons-Moll, G.: Stereo radiance fields (srf): Learning view synthesis for sparse views of novel scenes. In: Proceedings of the IEEE/CVF Conference on Computer Vision and Pattern Recognition. pp. 7911–7920 (2021) [4](#)
10. Debevec, P.E., Taylor, C.J., Malik, J.: Modeling and rendering architecture from photographs: A hybrid geometry-and image-based approach. In: SIGGRAPH (1996) [4](#)
11. Dosovitskiy, A., Fischer, P., Ilg, E., Hausser, P., Hazirbas, C., Golkov, V., Van Der Smagt, P., Cremers, D., Brox, T.: FlowNet: Learning optical flow with convolutional networks. In: Proceedings of the IEEE international conference on computer vision. pp. 2758–2766 (2015) [5](#)
12. Efros, A.A., Freeman, W.T.: Image quilting for texture synthesis and transfer. In: Seminal Graphics Papers: Pushing the Boundaries, Volume 2, pp. 571–576 (2023) [2](#), [4](#)
13. Efros, A.A., Leung, T.K.: Texture synthesis by non-parametric sampling. In: Proceedings of the seventh IEEE international conference on computer vision. vol. 2, pp. 1033–1038. IEEE (1999) [2](#), [4](#)
14. Fang, J., Wang, J., Zhang, X., Xie, L., Tian, Q.: Gaussianeditor: Editing 3d gaussians delicately with text instructions (2023) [5](#)
15. Gao, C., Gu, D., Zhang, F., Yu, Y.: Reconet: Real-time coherent video style transfer network. In: Computer Vision–ACCV 2018: 14th Asian Conference on Computer Vision, Perth, Australia, December 2–6, 2018, Revised Selected Papers, Part VI 14. pp. 637–653. Springer (2019) [4](#)
16. Gatys, L.A., Ecker, A.S., Bethge, M.: Image style transfer using convolutional neural networks. In: Proceedings of the IEEE conference on computer vision and pattern recognition. pp. 2414–2423 (2016) [2](#), [4](#), [9](#)

17. Gortler, S.J., Grzeszczuk, R., Szeliski, R., Cohen, M.F.: The Lumigraph. *SIGGRAPH* **96**(30) (1996) [4](#)
18. Guangcong, Chen, Z., Loy, C.C., Liu, Z.: Sparsenerf: Distilling depth ranking for few-shot novel view synthesis. *IEEE/CVF International Conference on Computer Vision (ICCV)* (2023) [4](#)
19. Gupta, A., Johnson, J., Alahi, A., Fei-Fei, L.: Characterizing and improving stability in neural style transfer. In: *Proceedings of the IEEE International Conference on Computer Vision*. pp. 4067–4076 (2017) [4](#)
20. Haque, A., Tancik, M., Efros, A.A., Holynski, A., Kanazawa, A.: Instruct-nerf2nerf: Editing 3d scenes with instructions. *arXiv preprint arXiv:2303.12789* (2023) [5](#)
21. Hedman, P., Philip, J., Price, T., Frahm, J.M., Drettakis, G., Brostow, G.: Deep Blending for Free-Viewpoint Image-Based Rendering. In: *SIGGRAPH Asia* (2018) [4](#)
22. Heigl, B., Koch, R., Pollefeys, M., Denzler, J., Van Gool, L.: Plenoptic Modeling and Rendering from Image Sequences taken by a Hand Held Camera. In: *GCPR* (1999) [4](#)
23. Höllein, L., Johnson, J., Nießner, M.: Stylemesh: Style transfer for indoor 3d scene reconstructions. In: *Proceedings of the IEEE/CVF Conference on Computer Vision and Pattern Recognition*. pp. 6198–6208 (2022) [5](#)
24. Hu, S.M., Liang, D., Yang, G.Y., Yang, G.W., Zhou, W.Y.: Jittor: a novel deep learning framework with meta-operators and unified graph execution. *Science China Information Sciences* **63**(222103), 1–21 (2020) [9](#)
25. Huang, H., Wang, H., Luo, W., Ma, L., Jiang, W., Zhu, X., Li, Z., Liu, W.: Real-time neural style transfer for videos. In: *Proceedings of the IEEE conference on computer vision and pattern recognition*. pp. 783–791 (2017) [4](#)
26. Huang, H.P., Tseng, H.Y., Saini, S., Singh, M., Yang, M.H.: Learning to stylize novel views. In: *Proceedings of the IEEE/CVF International Conference on Computer Vision*. pp. 13869–13878 (2021) [2](#), [3](#), [5](#), [9](#), [10](#), [11](#)
27. Huang, X., Belongie, S.: Arbitrary style transfer in real-time with adaptive instance normalization. In: *Proceedings of the IEEE international conference on computer vision*. pp. 1501–1510 (2017) [2](#), [4](#), [7](#), [8](#), [9](#), [10](#)
28. Huang, Y.H., He, Y., Yuan, Y.J., Lai, Y.K., Gao, L.: Stylizednerf: consistent 3d scene stylization as stylized nerf via 2d-3d mutual learning. In: *Proceedings of the IEEE/CVF Conference on Computer Vision and Pattern Recognition*. pp. 18342–18352 (2022) [2](#), [5](#), [6](#), [8](#), [9](#), [10](#), [11](#)
29. Hwang, I., Kim, H., Kim, Y.M.: Text2scene: Text-driven indoor scene stylization with part-aware details (2023) [5](#)
30. Ioannou, E., Maddock, S.: Depth-aware neural style transfer using instance normalization. *arXiv preprint arXiv:2203.09242* (2022) [4](#)
31. Johnson, J., Alahi, A., Fei-Fei, L.: Perceptual losses for real-time style transfer and super-resolution. In: *Computer Vision—ECCV 2016: 14th European Conference, Amsterdam, The Netherlands, October 11–14, 2016, Proceedings, Part II* 14. pp. 694–711. Springer (2016) [2](#), [4](#)
32. Jung, H., Nam, S., Sarafianos, N., Yoo, S., Sorkine-Hornung, A., Ranjan, R.: Geometry transfer for stylizing radiance fields (2024) [5](#)
33. Kerbl, B., Kopanas, G., Leimkühler, T., Drettakis, G.: 3d gaussian splatting for real-time radiance field rendering. *ACM Transactions on Graphics* **42**(4) (July 2023), <https://repo-sam.inria.fr/fungraph/3d-gaussian-splatting/> [3](#), [4](#), [5](#), [6](#), [9](#)
34. Kingma, D.P., Ba, J.: Adam: A method for stochastic optimization (2017) [9](#)



35. Knapitsch, A., Park, J., Zhou, Q.Y., Koltun, V.: Tanks and temples: Benchmarking large-scale scene reconstruction. *ACM Transactions on Graphics* **36**(4) (2017) [8](#)
36. Knapitsch, A., Park, J., Zhou, Q.Y., Koltun, V.: Tanks and temples: Benchmarking large-scale scene reconstruction. *ACM Transactions on Graphics (ToG)* **36**(4), 1–13 (2017) [10](#)
37. Kwatra, V., Schödl, A., Essa, I., Turk, G., Bobick, A.: Graphcut textures: Image and video synthesis using graph cuts. *Acm transactions on graphics (tog)* **22**(3), 277–286 (2003) [2](#), [4](#)
38. Lee, J.C., Rho, D., Sun, X., Ko, J.H., Park, E.: Compact 3d gaussian representation for radiance field. *arXiv preprint arXiv:2311.13681* (2023) [8](#)
39. Levoy, M., Hanrahan, P.: Light field rendering. In: *SIGGRAPH* (1996) [4](#)
40. Li, C., Wand, M.: Precomputed real-time texture synthesis with markovian generative adversarial networks. In: *Computer Vision–ECCV 2016: 14th European Conference, Amsterdam, The Netherlands, October 11–14, 2016, Proceedings, Part III* 14. pp. 702–716. Springer (2016) [4](#)
41. Li, W., Wu, T., Zhong, F., Oztireli, C.: Arf-plus: Controlling perceptual factors in artistic radiance fields for 3d scene stylization (2023) [5](#)
42. Li, Z., Müller, T., Evans, A., Taylor, R.H., Unberath, M., Liu, M.Y., Lin, C.H.: Neuralangelo: High-fidelity neural surface reconstruction. In: *IEEE Conference on Computer Vision and Pattern Recognition (CVPR)* (2023) [3](#)
43. Liu, K., Zhan, F., Chen, Y., Zhang, J., Yu, Y., Saddik, A.E., Lu, S., Xing, E.: Stylerf: Zero-shot 3d style transfer of neural radiance fields (2023) [2](#), [5](#), [9](#), [10](#), [11](#)
44. Liu, X.C., Cheng, M.M., Lai, Y.K., Rosin, P.L.: Depth-aware neural style transfer. In: *Proceedings of the symposium on non-photorealistic animation and rendering*. pp. 1–10 (2017) [4](#)
45. Martin-Brualla, R., Radwan, N., Sajjadi, M.S., Barron, J.T., Dosovitskiy, A., Duckworth, D.: Nerf in the wild: Neural radiance fields for unconstrained photo collections. In: *Proceedings of the IEEE/CVF Conference on Computer Vision and Pattern Recognition*. pp. 7210–7219 (2021) [6](#)
46. Mescheder, L., Oechsle, M., Niemeyer, M., Nowozin, S., Geiger, A.: Occupancy networks: Learning 3d reconstruction in function space. In: *Proceedings IEEE Conf. on Computer Vision and Pattern Recognition (CVPR)* (2019) [3](#)
47. Metzger, G., Richardson, E., Patashnik, O., Giryas, R., Cohen-Or, D.: Latent-nerf for shape-guided generation of 3d shapes and textures (2022) [5](#)
48. Michel, O., Bar-On, R., Liu, R., Benaim, S., Hanocka, R.: Text2mesh: Text-driven neural stylization for meshes (2021) [5](#)
49. Mildenhall, B., Srinivasan, P.P., Ortiz-Cayon, R., Kalantari, N.K., Ramamoorthi, R., Ng, R., Kar, A.: Local light field fusion: Practical view synthesis with prescriptive sampling guidelines. *ACM Transactions on Graphics (TOG)* **38**(4), 1–14 (2019) [2](#), [10](#)
50. Mildenhall, B., Srinivasan, P.P., Tancik, M., Barron, J.T., Ramamoorthi, R., Ng, R.: Nerf: Representing scenes as neural radiance fields for view synthesis. *Communications of the ACM* **65**(1), 99–106 (2021) [2](#), [3](#), [4](#), [5](#), [6](#)
51. Moreau, A., Song, J., Dharmo, H., Shaw, R., Zhou, Y., Pérez-Pellitero, E.: Human gaussian splatting: Real-time rendering of animatable avatars (2023) [2](#)
52. Mu, F., Wang, J., Wu, Y., Li, Y.: 3d photo stylization: Learning to generate stylized novel views from a single image. In: *Proceedings of the IEEE/CVF Conference on Computer Vision and Pattern Recognition*. pp. 16273–16282 (2022) [5](#)
53. Müller, T.: tiny-cuda-nn (4 2021), <https://github.com/NVlabs/tiny-cuda-nn> [8](#)

54. Müller, T., Evans, A., Schied, C., Keller, A.: Instant neural graphics primitives with a multiresolution hash encoding. *ACM Transactions on Graphics (ToG)* **41**(4), 1–15 (2022) [3](#), [4](#), [6](#), [8](#)
55. Nguyen-Ha, P., Huynh, L., Rahtu, E., Matas, J., Heikkil, J., et al.: Cascaded and generalizable neural radiance fields for fast view synthesis. *IEEE Transactions on Pattern Analysis and Machine Intelligence* (2023) [4](#)
56. Nguyen-Phuoc, T., Liu, F., Xiao, L.: Snerf: Stylized neural implicit representations for 3d scenes (2022) [5](#)
57. Niemeyer, M., Barron, J.T., Mildenhall, B., Sajjadi, M.S.M., Geiger, A., Radwan, N.: Regnerf: Regularizing neural radiance fields for view synthesis from sparse inputs (2021) [3](#), [4](#)
58. Niklaus, S., Liu, F.: Softmax splatting for video frame interpolation (2020) [10](#)
59. Niklaus, S., Mai, L., Yang, J., Liu, F.: 3d ken burns effect from a single image (2019) [2](#)
60. Pang, H., Zhu, H., Kortylewski, A., Theobalt, C., Habermann, M.: Ash: Animatable gaussian splats for efficient and photoreal human rendering (2023) [2](#)
61. Pang, H.W., Hua, B.S., Yeung, S.K.: Locally stylized neural radiance fields (2023) [5](#)
62. Park, J.J., Florence, P., Straub, J., Newcombe, R., Lovegrove, S.: Deepsdf: Learning continuous signed distance functions for shape representation (2019) [3](#)
63. Peng, S., Niemeyer, M., Mescheder, L., Pollefeys, M., Geiger, A.: Convolutional occupancy networks. In: *Computer Vision – ECCV 2020. Lecture Notes in Computer Science*, 12348, vol. 3, pp. 523–540. Springer, Cham (Aug 2020). [https://doi.org/10.1007/978-3-030-58580-8\\_31](https://doi.org/10.1007/978-3-030-58580-8_31) [3](#)
64. Qian, S., Kirschstein, T., Schoneveld, L., Davoli, D., Giebenhain, S., Nießner, M.: Gaussianavatars: Photorealistic head avatars with rigged 3d gaussians (2023) [2](#)
65. Radford, A., Kim, J.W., Hallacy, C., Ramesh, A., Goh, G., Agarwal, S., Sastry, G., Askell, A., Mishkin, P., Clark, J., et al.: Learning transferable visual models from natural language supervision. In: *International conference on machine learning*. pp. 8748–8763. PMLR (2021) [8](#), [9](#)
66. Reiser, C., Peng, S., Liao, Y., Geiger, A.: Kilonerf: Speeding up neural radiance fields with thousands of tiny mlps (2021) [3](#), [4](#)
67. Riegler, G., Koltun, V.: Free view synthesis. In: *Computer Vision–ECCV 2020: 16th European Conference, Glasgow, UK, August 23–28, 2020, Proceedings, Part XIX 16*. pp. 623–640. Springer (2020) [4](#)
68. Saleh, B., Elgammal, A.: Large-scale classification of fine-art paintings: Learning the right metric on the right feature (2015) [10](#)
69. Schwarz, K., Sauer, A., Niemeyer, M., Liao, Y., Geiger, A.: Voxgraf: Fast 3d-aware image synthesis with sparse voxel grids (2022) [3](#)
70. Seitz, S.M., Dyer, C.R.: View Morphing. *SIGGRAPH* (1996) [4](#)
71. Shin, D., Ren, Z., Sudderth, E.B., Fowlkes, C.C.: 3d scene reconstruction with multi-layer depth and epipolar transformers (2019) [2](#)
72. Simonyan, K., Zisserman, A.: Very deep convolutional networks for large-scale image recognition. *arXiv preprint arXiv:1409.1556* (2014) [4](#), [8](#), [9](#)
73. Sitzmann, V., Thies, J., Heide, F., Nießner, M., Wetzstein, G., Zollhöfer, M.: Deepvoxels: Learning persistent 3d feature embeddings. In: *CVPR* (2019) [4](#)
74. Sitzmann, V., Zollhöfer, M., Wetzstein, G.: Scene Representation Networks: Continuous 3D-Structure-Aware Neural Scene Representations. In: *NeurIPS* (2019) [4](#)
75. Song, H., Choi, S., Do, H., Lee, C., Kim, T.: Blending-nerf: Text-driven localized editing in neural radiance fields (2023) [5](#)

76. Teed, Z., Deng, J.: Raft: Recurrent all-pairs field transforms for optical flow (2020) [10](#)
77. Tulsiani, S., Gupta, S., Fouhey, D., Efros, A.A., Malik, J.: Factoring shape, pose, and layout from the 2d image of a 3d scene (2018) [2](#)
78. Ulyanov, D., Vedaldi, A., Lempitsky, V.: Improved texture networks: Maximizing quality and diversity in feed-forward stylization and texture synthesis. In: Proceedings of the IEEE conference on computer vision and pattern recognition. pp. 6924–6932 (2017) [4](#)
79. Wang, C., Jiang, R., Chai, M., He, M., Chen, D., Liao, J.: Nerf-art: Text-driven neural radiance fields stylization (2022) [5](#)
80. Wang, W., Yang, S., Xu, J., Liu, J.: Consistent video style transfer via relaxation and regularization. IEEE Transactions on Image Processing **29**, 9125–9139 (2020) [4](#)
81. Wei, L.Y., Levoy, M.: Fast texture synthesis using tree-structured vector quantization. In: Proceedings of the 27th annual conference on Computer graphics and interactive techniques. pp. 479–488 (2000) [2, 4](#)
82. Wiles, O., Gkioxari, G., Szeliski, R., Johnson, J.: Synsin: End-to-end view synthesis from a single image (2020) [2](#)
83. Wimbauer, F., Yang, N., Rupprecht, C., Cremers, D.: Behind the scenes: Density fields for single view reconstruction (2023) [4](#)
84. Xu, S., Li, L., Shen, L., Lian, Z.: Desrf: Deformable stylized radiance field. 2023 IEEE/CVF Conference on Computer Vision and Pattern Recognition Workshops (CVPRW) pp. 709–718 (2023), <https://api.semanticscholar.org/CorpusID:259237546> [5](#)
85. Yu, A., Fridovich-Keil, S., Tancik, M., Chen, Q., Recht, B., Kanazawa, A.: Plenoxels: Radiance fields without neural networks (2021) [3, 4](#)
86. Yu, A., Ye, V., Tancik, M., Kanazawa, A.: pixelnerf: Neural radiance fields from one or few images (2021) [3, 4](#)
87. Zhang, K., Kolkin, N., Bi, S., Luan, F., Xu, Z., Shechtman, E., Snavely, N.: Arf: Artistic radiance fields (2022) [2, 5, 9, 11](#)
88. Zhang, R., Isola, P., Efros, A.A., Shechtman, E., Wang, O.: The unreasonable effectiveness of deep features as a perceptual metric. In: CVPR (2018) [9, 10](#)
89. Zhang, Y., He, Z., Xing, J., Yao, X., Jia, J.: Ref-npr: Reference-based non-photorealistic radiance fields for controllable scene stylization (2023) [5](#)
90. Zhang, Z., Liu, Y., Han, C., Pan, Y., Guo, T., Yao, T.: Transforming radiance field with lipschitz network for photorealistic 3d scene stylization (2023) [5](#)
91. Zheng, S., Zhou, B., Shao, R., Liu, B., Zhang, S., Nie, L., Liu, Y.: Gps-gaussian: Generalizable pixel-wise 3d gaussian splatting for real-time human novel view synthesis (2023) [2](#)
92. Zitnick, C.L., Kang, S.B., Uyttendaele, M., Winder, S., Szeliski, R.: High-quality video view interpolation using a layered representation. SIGGRAPH **23**(3) (2004) [4](#)